

## Electronic Supplementary Information

### Sulfide bornite thermoelectric material: natural mineral with ultralow thermal conductivity

Pengfei Qiu,<sup>ab</sup> Tiansong Zhang,<sup>a</sup> Yuting Qiu,<sup>a</sup> Xun Shi,<sup>\*ab</sup> and Lidong Chen<sup>\*ab</sup>

<sup>a</sup> State Key Laboratory of High Performance Ceramics and Superfine Microstructure, Shanghai Institute of Ceramics, Chinese Academy of Sciences, 1295 Dingxi Road, Shanghai 200050, China.

<sup>b</sup> CAS Key Laboratory of Materials for Energy Conversion, Shanghai Institute of Ceramics, Chinese Academy of Sciences, Shanghai, 200050, China.

#### Physical parameters calculation details:

The average sound velocity is calculated by

$$v_{avg} = \frac{2\pi\Theta_D k_B}{h(6\pi^2 n)^{1/3}} \quad (1)$$

where  $\Theta_D$  is the Debye temperature,  $k_B$  is the Boltzmann constant,  $h$  is the Planck constant, and  $n$  is the number of atoms per unit volume.<sup>1</sup> The Grüneisen parameter, which is a direct measure of the anharmonicity of the bonds in a solid,<sup>2</sup> can be estimated through the relationship<sup>3</sup>

$$\kappa_L = A \frac{M_{avg} \Theta_D^3 \delta}{\gamma^2 n^{2/3} T} \quad (2)$$

where  $\kappa_L$  is the lattice thermal conductivity,  $M_{avg}$  is the average mass of the atoms in the crystal,  $\delta^3$  is the volume per atom,  $n$  is the number of atoms in the primitive unit cell ( $n = 10$  for  $\text{Cu}_5\text{FeS}_4$ ), and  $A$  is a collection of physical constants ( $A = 3.1 \times 10^{-6}$  if  $\kappa$  is in  $\text{Wm}^{-1}\text{K}^{-1}$ ,  $M_{avg}$  in amu, and  $\delta$  in Angstroms).

## Electronic Supplementary Information

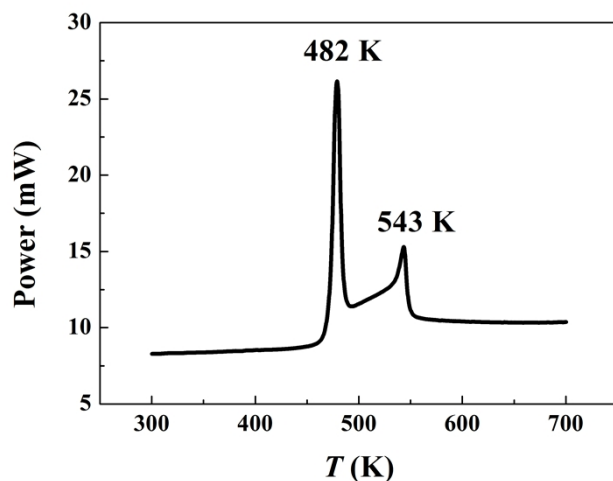


Figure S1. DSC scan profile for bornite  $\text{Cu}_5\text{FeS}_4$  between 300 and 700 K. The two exothermic peaks at the temperature of 482 K and 543 K imply the existence of two phase transitions over the measured temperature range.

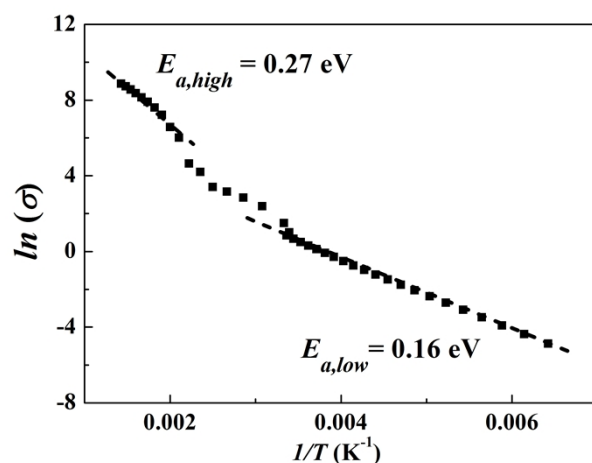


Figure S2.  $\ln(\sigma)$  as a function of  $1/T$  for Bornite. The dashed lines represent the fitting curves using the empirical relation,  $\sigma \sim \exp(-E_a/k_B T)$ .

## Electronic Supplementary Information

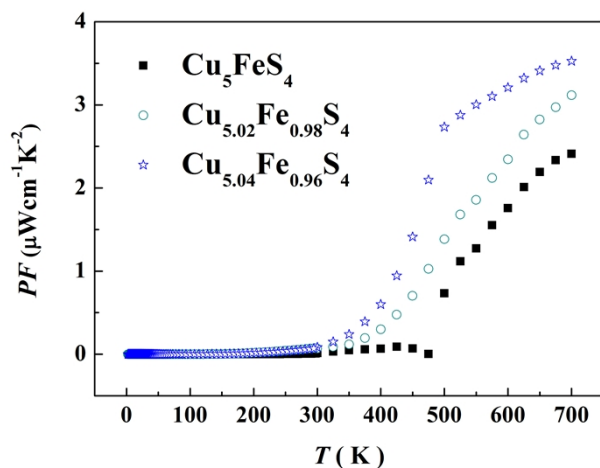


Figure S3. Temperature dependence of power factor ( $PF = S^2 \sigma$ ) for bornite samples.

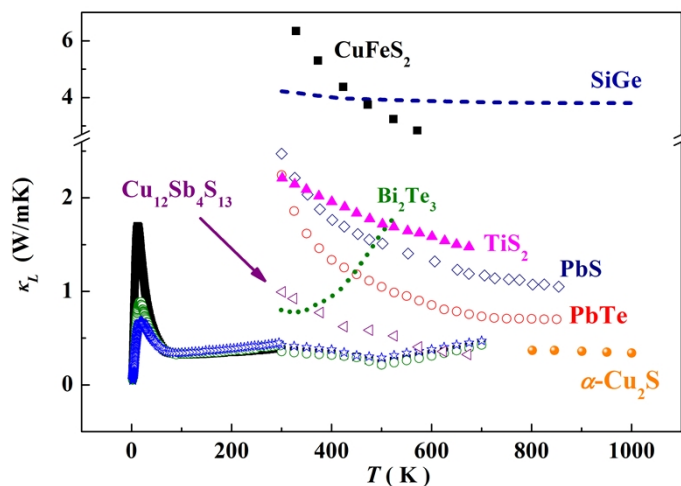


Figure S4. Temperature dependence of lattice thermal conductivities of bornite and some state-of-the-art TE materials such as  $\text{Bi}_2\text{Te}_3$ ,<sup>4</sup>  $\text{PbTe}$ ,<sup>5</sup> and  $\text{SiGe}$ <sup>6</sup> as well as the reported sulfides such as  $\text{TiS}_2$ ,<sup>7</sup>  $\text{PbS}$ ,<sup>8</sup>  $\text{CuFeS}_2$ ,<sup>9</sup>  $\text{Cu}_{12}\text{Sb}_4\text{S}_{13}$ ,<sup>10</sup> and  $\alpha\text{-Cu}_2\text{S}$ .<sup>11</sup>

## Electronic Supplementary Information

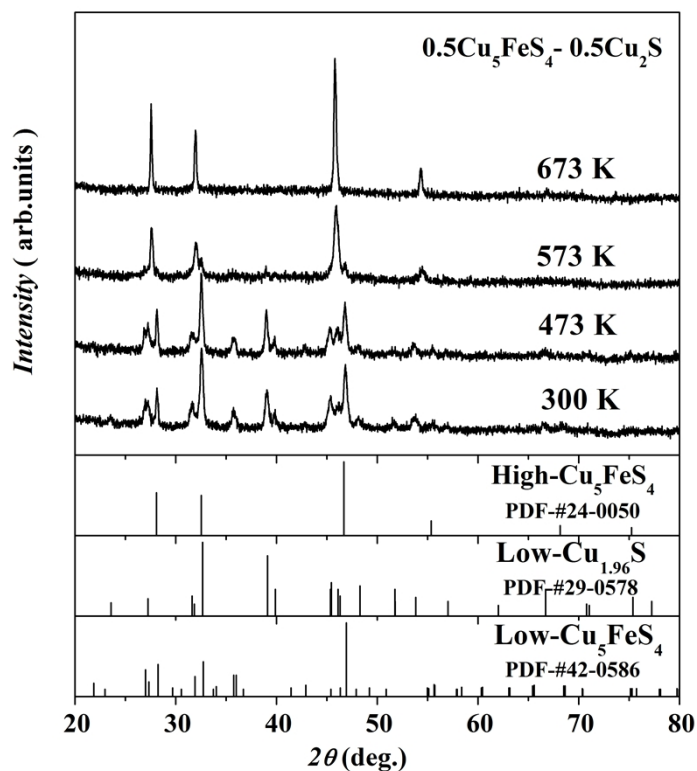


Figure S5. XRD diffraction patterns of  $0.5\text{Cu}_8\text{S}_4-0.5\text{Cu}_5\text{Fe}\square_2\text{S}_4$  solid solution collected at 300 K, 473 K, 573 K, and 673 K. At 300 K, the solid solution sample consists of two phases, orthorhombic  $\text{Cu}_5\text{FeS}_4$  and tetragonal  $\text{Cu}_{1.96}\text{S}$ . These two phases gradually transfer to cubic phase when increasing temperature. The diffraction peaks at 673 K for  $0.5\text{Cu}_8\text{S}_4-0.5\text{Cu}_5\text{Fe}\square_2\text{S}_4$  solid solution shift to the low angle as compared with those for high cubic phase of  $\text{Cu}_5\text{FeS}_4$  (PDF-#24-0050) because the lattice parameter of  $\text{Cu}_2\text{S}$  ( $\sim 5.707 \text{ \AA}$ ) is larger than that of  $\text{Cu}_5\text{FeS}_4$  ( $\sim 5.5 \text{ \AA}$ ).

## Electronic Supplementary Information

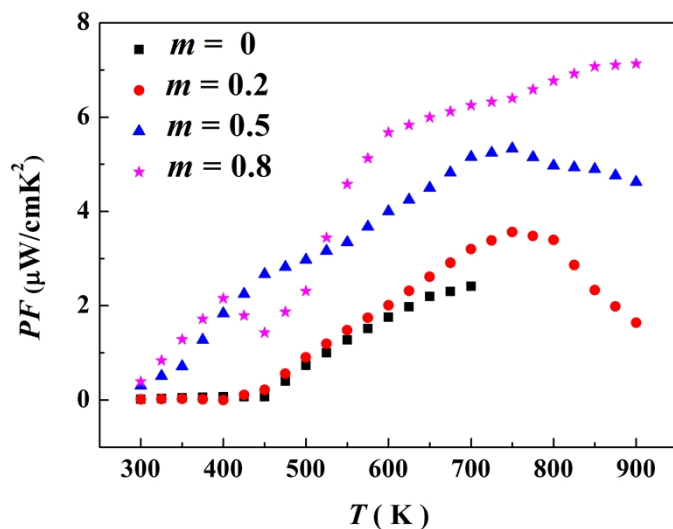


Figure S6. Temperature dependence of power factor ( $PF = S^2 \sigma$ ) for  $m\text{Cu}_8\text{S}_4-(1-m)\text{Cu}_5\text{Fe}\square_2\text{S}_4$  ( $m = 0, 0.2, 0.5, 0.8$ ).

### References

- [1] O. L. Anderson, *J. Phys. Chem. Solids* **1963**, *24*, 909.
- [2] H. J. Goldsmid, *Electronic Refrigeration*, London: Pion, **1986**.
- [3] D. T. Morelli, V. Jovovic, J. P. Heremans, *Phys. Rev. Lett.* **2008**, *101*, 035901.
- [4] B. Poudel, Q. Hao, Y. Ma, Y. Lan, A. Minnich, B. Yu, X. Yan, D. Wang, A. Muto, D. Vashaee, X. Chen, J. Liu, M. Dresselhaus, G. Chen, and Z. Ren, *Science* 2008, **320**, 634.
- [5] Y. Pei, X. Shi, A. Lalonde, H. Wang, L. Chen, and G. J. Snyder, *Nature* 2011, **473**, 66.
- [6] G. Joshi, H. Lee, Y. Lan, X. Wang, G. Zhu, D. Wang, R. Gould, D.C. Cuff, M.Y. Tang, M.S. Dresselhaus, G. Chen, and Z. Ren, *Nano Letter*, 2008, **8**, 4670.
- [7] M. Beaumale, T. Barbier, Y. Bréard, S. Hébert, Y. Kinemuchi, and E. Guilmeau, *J. Appl. Phys.* 2014, **115**, 043704.
- [8] H. Wang, E. Schechtel, Y. Pei, and G. J. Snyder, *Adv. Energy Mater.* 2013, **3**, 488.
- [9] J. Li, Q. Tan, and J-F. Li, *J. Alloys. Compd.* 2013, **551**, 143.
- [10] X. Lu, D. T. Morelli, Y. Xia, F. Zhou, V. Ozolins, H. Chi, X. Zhou, and C. Uher, *Adv. Energy Mater.* 2013, **3**, 342.

## Electronic Supplementary Information

[11] Y. He, T. Day, T. Zhang, H. Liu, X. Shi, L. Chen, and G. J. Snyder, *Adv. Mater.* 2014, **26**, 3974.